Biglycan regulates the expression and sarcolemmal localization of dystrobrevin, syntrophin, and nNOS

Mary Lynn Mercado,* Alison R. Amenta,* Hiroki Hagiwara,* Michael S. Rafii,* Beatrice E. Lechner,* Rick T. Owens,† David J. McQuillan,† Stanley C. Froehner,‡ and Justin R. Fallon*,[1]

*Department of Neuroscience, Brown University, Providence, Rhode Island, USA; †LifeCell Corporation, Branchburg, New Jersey, USA; and ‡Department of Physiology and Biophysics, University of Washington, Seattle, Washington, USA

ABSTRACT **The dystrophin-associated protein complex (DAPC) provides a linkage between the cytoskeleton and the extracellular matrix (ECM) and is also a scaffold for a host of signaling molecules. The constituents of the DAPC must be targeted to the sarcolemma in order to properly function. Biglycan is an ECM molecule that associates with the DAPC. Here, we show that biglycan null mice exhibit a mild dystrophic phenotype and display a selective reduction in the localization of α-dystrobrevin-1 and -2, α- and β1-syntrophin, and nNOS at the sarcolemma. Purified biglycan induces nNOS redistribution to the plasma membrane in cultured muscle cells. Biglycan protein injected into muscle becomes stably associated with the sarcolemma and ECM for at least 2 wk. This injected biglycan restores the sarcolemmal expression of α-dystrobrevin-1 and -2, and β1- and β2-syntrophin in biglycan null mice. We conclude that biglycan is important for the maintenance of muscle cell integrity and plays a direct role in regulating the expression and sarcolemmal localization of the intracellular signaling proteins dystrobrevin-1 and -2, α- and β1-syntrophin and nNOS.—Mercado, M. L., Amenta, A. R., Hagiwara, H., Rafii, M. S., Lechner, B., Owens, R. T., McQuillan, D. J., Froehner, S. C., Fallon, J. R. Biglycan regulates the expression and sarcolemmal localization of dystrobrevin, syntrophin, and nNOS. *FASEB J.* 20, E1075–E1085 (2006)**

Key Words: dystrophin-associated protein complex · α-dystrobrevin-2 · sarcoglycans · β1-syntrophin

The dystrophin-associated protein complex (DAPC) provides a critical link between the basal lamina and the cytoskeleton in skeletal muscle. It is comprised of three subcomplexes: dystrophin-dystroglycans (α-, β-); sarcoglycans (α-, β-, γ- δ-)-sarcospan; and the cytosolic dystrobrevin-syntrophin-nNOS (1,2). Dystrophin binds actin and the cytoplasmic tail of β-dystroglycan. α-Dystroglycan in turn connects β-dystroglycan with the ECM molecules laminin, agrin, perlecan, and biglycan (2,3). The maintenance of a linkage between the ECM and the cytoskeleton is important for maintaining skeletal muscle function and stability. At the cellular level, mutations in genes that encode for proteins of the DAPC cause destabilization of the DAPC, loss of membrane integrity, and degeneration of muscle fibers (4, 5).

We previously demonstrated that the ECM molecule biglycan is expressed on the skeletal muscle surface and binds to the DAPC protein α-dystroglycan (3). Biglycan is a member of the small leucine-rich repeat proteoglycan (SLRP) family. It contains within its 38 kDa polypeptide core sequence 10 leucine-rich repeats flanked by two cysteine-rich domains, and two glycosaminoglycan (GAG) attachment sites at its NH_2 terminus. Biglycan-deficient mice have been shown to display decreased growth rates as well as reduced bone mass (first detected at 6 mo of age) and premature osteoarthritis (6, 7). Muscle expresses both a "proteoglycan" (PG) form and a "core" polypeptide that lacks the GAG chains. Biglycan has been shown to play a role in skeletal muscle development and regeneration. It becomes up-regulated during muscle fiber regeneration, and mice deficient in biglycan display delayed regeneration after injury (8). In addition, mice overexpressing biglycan demonstrate aberrant eyelid muscle development (9). However, it is not known how extracellular biglycan affects processes that rely on signaling inside the muscle cell and how biglycan influences the composition of the DAPC complex.

Here we show that adult biglycan null mice are mildly dystrophic, displaying increased muscle fiber degeneration and regeneration, abnormal fiber size distribution and muscle membrane weakness. Examination of DAPC elements revealed a selective reduction in the localization of α-dystrobrevin-1 and -2, α- and β1-syntrophin, and nNOS to the sarcolemma. Exogenous biglycan induced the relocalization of nNOS from the cytosol to the plasma membrane in cultured biglycan null muscle cells. Finally, intramuscular (i.m.) injection of recombinant biglycan restored the expression of

[1]Correspondence: Department of Neuroscience, Brown University, 190 Thayer St., Box 1953, Providence, RI 02912 USA. E-mail: Justin_Fallon@brown.edu

doi: 10.1096/fj.05–5124fje

α-dystrobrevin-1, α-dystrobrevin-2, and β1-syntrophin to the sarcolemma of biglycan null mice. Thus, biglycan is important for the maintenance of muscle cell integrity and plays a direct role in regulating the expression and sarcolemmal localization of the intracellular DAPC signaling proteins α-dystrobrevin-1 and -2, α- and β1-syntrophin, and nNOS.

MATERIALS AND METHODS

Expression and purification of recombinant biglycan

Recombinant biglycan was produced using a stable transfected 293-EBNA cell line. The cell line was created by transferring a biglycan polyhistidine fusion construct, originally created for expression using a vaccinia virus expression system into the pCEP4 (Invitrogen Corporation, Carlsbad, CA, USA) expression vector. The resulting plasmid was transfected into 293-EBNA cells and stable expressing cells selected by culturing in the presence of hygromycin B. Following amplification, cells were seeded into a Celligen Plus bioreactor (New Brunswick Scientific, Edison, NJ, USA) containing 100 g Fibra-Cel disks and grown to saturation. Protein production was initiated by replacing the culture media with serum free Dulbecco's modified Eagle medium (DMEM). Conditioned media was collected every 48 h with fresh media being added back to the bioreactor. Following concentration of the conditioned media using a Pellicon 2 Tangential Flow system (Millipore Corporation, Bedford, MA, USA), recombinant biglycan was purified using nickel chelating chromatography and elution with a gradient of 0–250 mM imidazole in 20 mM Tris-HCl, 500 mM NaCl, 0.2% CHAPS, pH 8.0. Biglycan polypeptide with "proteoglycan" and with "core" GAG side chains was subsequently separated from proteoglycan after anion exchange chromatography on Q-Sepharose and elution with a linear gradient of 0.15–2 M NaCl in PBS, 0.2% CHAPS. Note that both forms are N-glycosylated (10).

Antibodies

The following primary antibodies were used: anti-biglycan (clones 2A5 and 4C6) (Creely et al., unpublished results), pan-specific anti-dystrobrevin (BD Transduction Laboratories) (San Jose, CA, USA), isoform-specific syntrophin antibodies SYN259 (α-syntrophin), SYN29 (β2-syntrophin) and SYN37 (β1-syntrophin) (11), dystrobrevin antibodies 638 (α-dystrobrevin–1), and DB2 (α-dystrobrevin-2) (12), anti-nNOS (Immunostar, Hudson, WI, USA), anti-6–10 (dystrophin) (a generous gift from Timothy J. Byers and Louis M. Kunkel (Harvard Medical School and Children's Hospital, Boston, MA, USA), anti-merosin (Alexis Biochemicals, San Diego, CA, USA) and NCL-dys2 (dystrophin), NCL-g-sarc (γ-sarcoglycan), NCL-b-sarc (β-sarcoglycan), and NCL-a-sarc (α-sarcoglycan) (NovoCastra, Newcastle on Tyne, UK). The following secondary antibodies were used: Alexa 488-goat anti-rabbit IgG, Alexa 488-goat anti-mouse IgG (Molecular Probes, Eugene, OR, USA), Cy3-goat anti-rabbit IgG (Jackson Immunoresearch, West Grove, PA, USA) horseradish peroxidase-goat anti-rabbit IgG, and horseradish peroxidase-goat anti-mouse IgG (Amersham, Piscataway, NJ, USA).

Biglycan antibody (Ab) production

A monoclonal antibody capable of detecting biglycan immunohistochemically was produced. Adult biglycan null mice were injected with vaccinia virus/T7 bacteriophage system-expressed core and proteoglycan forms of biglycan (13) in Titermax Gold adjuvant (Sigma, St. Louis, MO, USA). Six booster injections of biglycan core and proteoglycan were performed. Splenocytes were fused by Green Mountain Antibodies (Burlington, VT, USA) and specific Ab production was tested via immunohistochemistry on quadriceps sections from wild-type and biglycan null mice. Hybridomas secreting antibodies that immunostained wild-type but not biglycan-deficient muscle sections were considered positive and were subcloned. Further characterization showed that these antibodies recognized purified biglycan in solid-phase binding assays. Monoclonal antibodies 2A5 and 4C6 were used in the present studies.

Skeletal muscle membrane preparations

Quadriceps from 5-wk-old mice were homogenized in dissection buffer containing 0.3 M sucrose, 35 mM Tris (pH 7.4), 10 mM EDTA, 10 mM EGTA, a protease inhibitor cocktail (Roche Applied Science, Indianapolis, IN, USA), and sodium azide. Samples were sonicated on ice for 3 × 10 s and centrifuged at 7000 *g* at 4°C for 20 min. Solid KCl was added to a final concentration of 0.6 M and the samples were centrifuged 7000 *g* for 20 min. The membranes were then collected by centrifugation for 140,000 *g* for 60 min at 4°C. Protein concentrations were determined by the bicinchoninic acid (Pierce, Rockford, IL, USA) protein concentration assay.

Western blot analysis

Proteins were transferred from SDS-PAGE gels to nitrocellulose membranes in transfer buffer at 100 V for 1 h at 4°C. Membranes were blocked in TBS, 0.1% Tween-20, 4.0% normal goat serum, 5.0% milk for 1 h at room temperature and incubated with primary Ab in blocking buffer overnight at 4°C. Membranes were washed and incubated for 1 h at room temperature with goat anti-rabbit or anti-mouse IgG conjugated to horseradish peroxidase (Amersham Biosciences) diluted 1:1000 in blocking buffer. After washing, bound Ab was detected using enhanced chemiluminescence according to the manufacturer's protocol (Amersham).

Biglycan null mice

The biglycan null mice used were generated by inserting the PGK-*neo* cassette from the pPNT vector into exon 2 at the *Tth*111I site as described (6). The original C57BL/6 background mice were rederived and then backcrossed to C3H for several generations to create congenic animals (14) and were obtained from Jackson Labs (Bar Harbor, ME, USA). Five- or 8-wk-old wild-type and biglycan-deficient mice on C3H background were utilized in this set of experiments. Similar results were observed at both ages. (In preliminary experiments, we observed that wild-type and biglycan null littermates on the C57BL/6 background gave results indistinguishable from those seen with the C3H background animals.) The animals were housed at room temperature with a 24 h night-day cycle and fed with pellets and water *ad libitum*. All protocols were conducted under strict accordance and with the formal approval of Brown University's Institutional Animal Care and Use Committee.

Quantitative polymerase chain reaction (PCR) analysis

RNA extraction from p35 quadriceps muscle was performed using the Trizol method (Invitrogen, Carlsbad, CA, Carlsbad,

CA, USA). Purified RNA was converted to cDNA using the Superscript III First-Strand Synthesis System Kit (Invitrogen, Carlsbad, CA, USA). qPCR reactions were performed using the SYBR-Green method (Invitrogen) on the ABI PRISM 7300 real-time thermocycler. Primers were designed using DS Gene primer design software (Accelrys, San Diego, CA, USA). ATP synthase was used for normalization. Data analysis was performed using the standard curve method (15). All experiments were performed in triplicate using three pairs of wild-type and biglycan null mice.

The primers used were ATPSase forward: 5′-TGG GAA AAT CGG ACT CTT TG-3′; ATPSase reverse: 5′-AGT AAC CAC chloroamphenicol acetyltransferase (CAT) GGG CTT TG-3′; α-syntrophin forward, 5′-CTG AAG AGG ATC GTT CAT C-3′; α-syntrophin reverse: 5′-TCA GGC TGG TCT CTG AG-3′; β1-syntrophin forward, 5′-GAA CAG AGA GGC GAC TTG CC-3′; β1-syntrophin reverse: 5′-chloroamphenicol acetyltransferase GTG ACT CCT TAA acetyl-coenzyme A carboxylase (ACC) TG-3′; β2-syntrophin forward: 5′-GCA ACA ACA AAG AAG C-3′; β2-syntrophin reverse: 5′CCT GTT GTG GTC CAG CAG TG-3′; α-dystrobrevin-1 forward, 5′-TGA AGA ACA CAG GCT GAT CG-3′; α-dystrobrevin-1 reverse: 5′-GCA TCG ATG GTG AAG GAG AT-3′; α-dystrobrevin-2 forward, 5′-CCT CTT GTC TTG TTC CCT GTG-3′; α-dystrobrevin-2 reverse: 5′-CAG CGC CCT AAA AAC AGA AA-3′; nNOS forward, 5′-GGG CAA ACA GTC TCC TAC CA-3′; nNOS reverse: 5′-AGG GTG TCA GTG AGG ACC AC-3′.

Evans blue dye staining and serum creatine kinase

A 10 mg/ml solution of Evans blue dye in PBS was injected into the tail vein of wild-type, biglycan-null, and *mdx* mice. Quadriceps muscles were collected 3–6 h later and cryosectioned. Evans blue dye-positive myofibers were observed under the fluorescent microscope using a rhodamine filter set. One hundred myofibers per section for each of three mice per genotype were counted. For serum creatine kinase measurements, blood was collected from anesthetized animals by retro-orbital bleed and clotted, and enzyme levels were measured using a commercial kit (Sigma).

Histology and immunohistochemistry

Quadriceps femoris muscles were isolated and flash-frozen in liquid nitrogen-cooled isopentane. In all experiments 10 μm sections from age-matched, congenic *bgn* null and wild-type muscle were mounted on the same slide. Sections were postfixed with 4% freshly prepared paraformaldehyde for 5 min at room temperature, blocked in Vector blocking reagent for 1 h at room temperature, and incubated with the indicated primary Ab overnight at 4°C, followed by secondary Ab for 1 h at room temperature. The Vector M.O.M. Basic kit was used according to the manufacturer's protocol. Sections were mounted in Permafluor (Thermo Electron Corporation, Pittsburgh, PA, USA) and analyzed using confocal laser scanning microscopy (Leica TCS SP2 Acousto-Optical Beam Splitter (AOBS). No immunostaining was observed if nonimmune IgG or an irrelevant Ab were substituted for the first layer; controls also showed that the secondary antibodies were species-specific. All comparison images presented here were captured from sections of *bgn* null and wild-type muscle that had been mounted on the same slide. Images were acquired using Leica LCS acquisition software and imported into Adobe Photoshop. Sections were also observed using a Nikon (Melville, NY, USA) Eclipse E800 microscope and images acquired with Scanalytics (Fairfax, VA, USA) IP Lab Spectrum software.

Cell culture

The biglycan null immortalized muscle cell line was generated using established protocols (16). Biglycan null cells were grown to ~75% confluence on gelatin-coated Permanox chamberslides (Nalge Nunc, Naperville, IL, USA) at 33°C and 10% carbon dioxide in growth medium containing Dulbecco's modified Eagle's medium (DMEM) high glucose (Glc), 20% FBS, 2% chick embryo extract, 1% L-glutamine, 1% penicillin/streptomycin, and 1U INF-γ. Cells were differentiated for 4–9 days in medium containing DMEM high Glc, 5% horse serum, 1% L-glutamine, and 1% penicillin/streptomycin.

Immunocytochemistry

Differentiated biglycan null cells were incubated for 4 h at 33°C with 0.7 nM biglycan core. Acetylcholine (Ach) receptors were labeled with rhodamine-α-bungarotoxin for 30 min at 33°C. Further incubations were completed at room temperature and cells were rinsed in MEM-H after each step. Cells were fixed in 1% paraformaldehyde and permeabilized with 0.05% saponin. To detect nNOS, cells were incubated in primary Ab for 1 h, then incubated in goat-anti-mouse IgG Alexa 488 for 1 h. Cells were fixed with methanol for 5 min at –20°C and mounted in Vectashield Hard Set with 4′,6′-diamidino-2-phenylidole (Vector laboratories, Burlinghame, CA, USA). Images were acquired on a Nikon Eclipse E800 microscope using a 60 × objective. Based on the captured images, myotube segments were scored blind to condition on a 0–4 scale that was based on the extent of nNOS on the myotube surface as delineated by AChR localization. A segment with no surface-localized nNOS received a score of 0 and a segment with the greatest extent received a 4.

Intramuscular biglycan injections

Fifty μg of purified recombinant biglycan core in 50 μl 20 mM Tris, 0.5M NaCl, 0.2% CHAPS, pH 8.0/1.0% India ink was injected i.m. into the right quadriceps femoris of 2-wk-old biglycan null mice using a 29 1/2G insulin syringe (BD Biosciences, San Jose, CA, USA). Fifty μl of 20 mM Tris, 0.5M NaCl, 0.2% CHAPS, pH 8.0/1.0% India ink was injected into the left quadriceps femoris of each animal to serve as an internal control. The injected quadriceps were isolated 4, 7, 11, and 14 days after biglycan injection. The injections on 2-wk-old animals were performed using three *bgn* null litters. The increase in α-dystrobrevin-1, α-dystrobrevin-2, β1-syntrophin, and β2-syntrophin at 11 days after injection was seen in 4 out of 4 animals and the increase at 14 days after injection was observed in 4 out of 4 animals. No increase was observed in any of the vehicle-injected muscles.

For immunohistochemical labeling of injected muscle tissue, quadriceps femoris muscles were isolated and sectioned as described above. In all experiments, sections from vehicle- and biglycan-injected muscle from the same animal were mounted on the same slide. Sections were double-immunolabeled with antibiglycan monoclonal antibodies 2A5 or 4C6 and a rabbit polyclonal antibody against the specified dystrobrevin or syntrophin isoform or nNOS (see Antibodies). The secondary antibodies used for detection were Alexa Fluor 488-goat anti-mouse IgG and Cy3-goat anti-rabbit IgG both diluted 1:2000.

RESULTS

Biglycan null mice display a dystrophic phenotype

Mutations in any one of several DAPC components cause a wide range of muscular dystrophies (5, 17). Since biglycan binds to three DAPC components, α-dystroglycan, α-sarcoglycan, and γ-sarcoglycan (3) (M. S. Rafii, H. Hagiwara, and J. R. Fallon, unpublished results), we tested whether biglycan null mice display a dystrophic phenotype (**Fig. 1**). First, we performed the Evans blue dye uptake assay to determine whether muscle membrane integrity is compromised in the biglycan null mice. *Bgn* null, wild-type littermates, and dystrophin-null *mdx* mice were intravenously (i.v.) injected with Evans blue dye and the extent of uptake in skeletal muscle fibers was assessed after 6 h. Wild-type muscle cells exhibited little detectable dye permeability (<0.5% of cells), while >90% of *mdx* myofibers showed dye uptake (18) (Fig. 1*A*). *Bgn* null fibers displayed an intermediate pattern. One population of fibers was completely permeable and showed a uniform dye distribution (7.4%±1.3; n=3), while others showed a perimembranous distribution. This localization at the cell periphery was not observed in control muscles from wild-type littermates. Measurement of serum creatine kinase levels also indicated modest sarcolemmal permeability in the *bgn* null mice. We observed levels of 240 ± 43, 870 ± 104, and 6435 ± 385 for wild-type, *bgn* null, and mdx mice, respectively; U/L, ± SE, n = 3). Thus, a subpopulation of myofibers in *bgn* null mice shows evidence of leaky membranes and loss of sarcolemmal integrity.

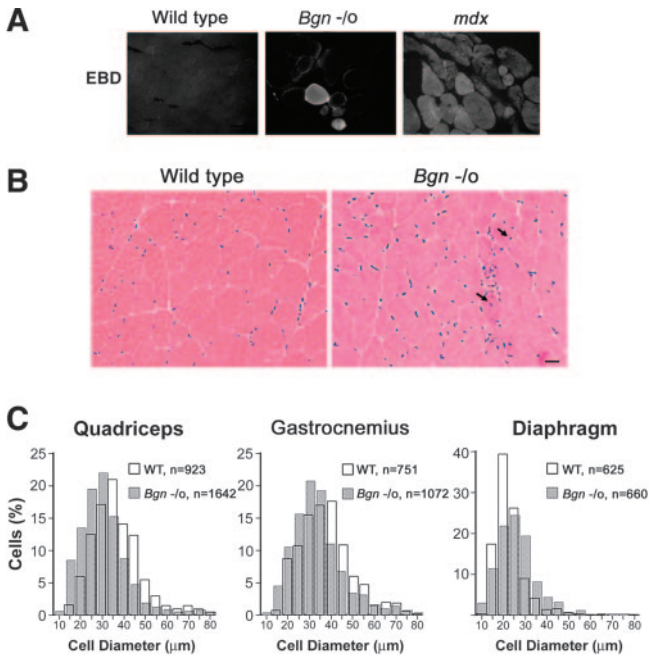

Figure 1. Dystrophic phenotype in *bgn* null mice. *A)* Evans blue dye (EBD) uptake. Wild-type and *bgn* null (*bgn*-/o) mice (8-wk-old) were i.v. injected with EBD and dye uptake into quadriceps femoris muscles was assessed 6 h later by fluorescence microscopy. A subset of *bgn* null muscle fibers exhibited complete dye permeation (7.4%±1.3; n=3), while other fibers displayed a perimembranous uptake. Essentially no uptake (<0.5% of fibers) was observed in muscle from wild-type animals, while >90% of dystrophin-null *mdx* fibers showed complete permeation. *B)* Hematoxylin and eosin-stained quadriceps femoris sections from wild-type and *bgn* -/o mice. *Bgn* null mice exhibit groups of muscle fibers with centrally nucleated nuclei (arrows) characteristic of cells that have regenerated in the adult animal. Central nuclei are rarely detected in the muscle fibers of wild-type animals. Scale bar = 10 μm. *C)* Distributions of cell diameters of wild-type and *bgn* null muscle fibers. Muscle fiber diameters from wild-type and *bgn* null quadriceps femoris, gastrocnemius, and diaphragm were measured and their distributions plotted. White bars represent wild-type (wild-type) cell diameters and gray bars represent *bgn*-/o cell diameters. The number of fibers counted per muscle type is indicated. *Bgn* null quadriceps and gastrocnemius fibers are smaller than wild-type, while *bgn* null diaphragm fibers display a wider size distribution.

We next examined the histology of the muscles from *bgn* null mice. As shown in Fig. 1*B*, the majority of fibers in *bgn* null muscle were similar to those in wild-type as judged by hematoxylin and eosin staining. However, a fraction of the myofibers in *bgn* null mice displayed centrally localized nuclei, a hallmark of regenerated fibers (5.08%±0.58 and 9.65%±1.34 in quadriceps and diaphragm, respectively). In contrast <0.5% of fibers in wild-type animals showed central nuclei. Similar percentages of centrally nucleated fibers were observed in quadriceps muscles from 4-, 12-, and 24-wk-old *bgn* knockouts (data not shown). We did not observe extensive mononuclear cell infiltration or fibrosis in the *bgn* null muscle.

Abnormal muscle is often characterized by an increased variability in fiber size. We therefore measured fiber diameters from quadriceps femoris, gastrocnemius, and diaphragm (Fig. 1*C*). In the quadriceps and gastrocnemius, *bgn* null fibers were smaller than wild-type fibers. The mean quadriceps fiber diameter in wild-type was 36.89 ± 3.88 μm vs. 30.56 ± 2.73 μm in the biglycan knockout. The mean gastrocnemius fiber diameter in wild-type was 38.14 ± 4.69 μm vs. 33.67 ± 3.52 μm in the biglycan knockout. On the other hand, the diaphragm of *bgn* null mice displayed a wider fiber size distribution (Fig. 1*C*). The mean fiber size diameter in wild-type diaphragm was 23.20 ± 3.08 μm vs. 27.89 μm ± 5.21 μm in *bgn* null diaphragm. Taken together, these results indicate that *bgn* null mice display a mild dystrophic phenotype.

Selective reduction of α-dystrobrevin, syntrophin, and nNOS expression at the sarcolemma of *bgn* null mice

We next compared the expression of individual DAPC proteins in adult wild-type and *bgn* null mice. In all cases we compared *bgn* null mice to either normal littermates or to congenic, age-matched wild-type animals. The results were consistent between both sets of animals. We first examined the expression levels of dystrophin, the major transmembrane complexes, and the most prominent basal lamina ligand of the DAPC,

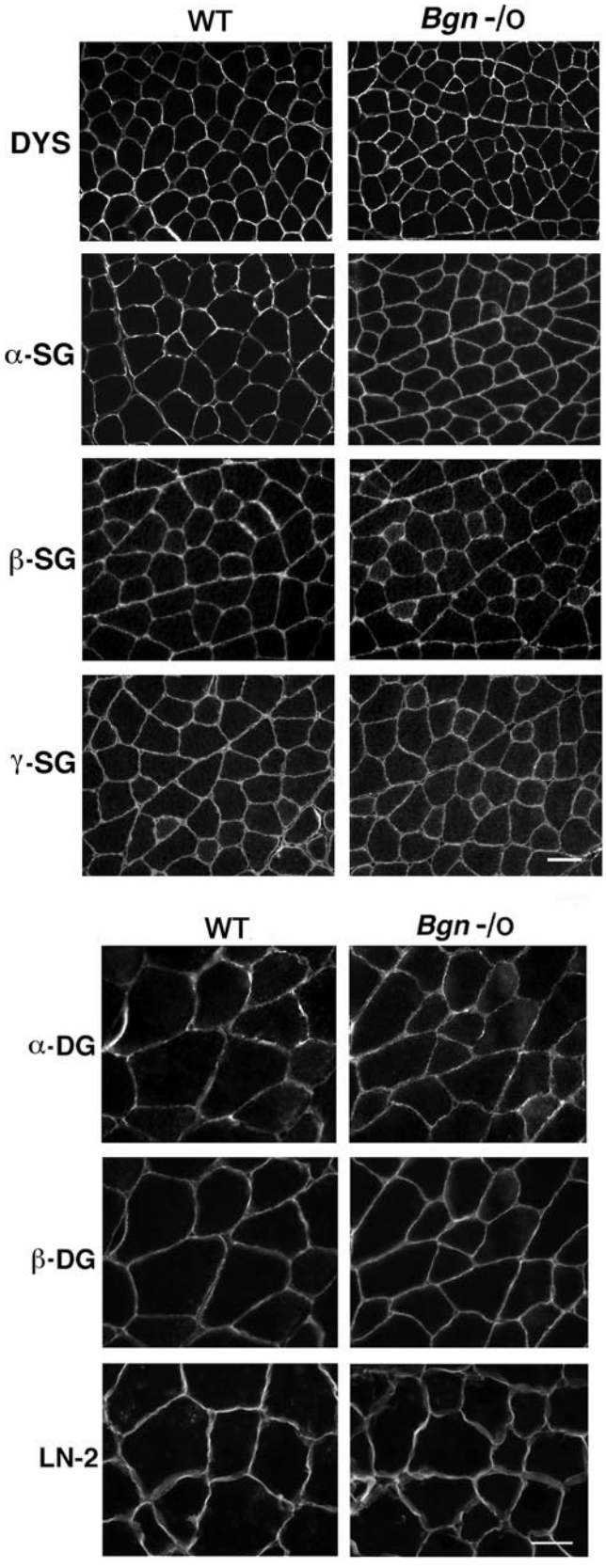

Figure 2. Expression of dystrophin, sarcoglycans, dystroglycans, and laminin α2 in wild-type and *bgn* null skeletal muscle. A comparison of the expression of DAPC proteins in skeletal muscle of wild-type and *bgn* null (*bgn* -/o) animals. Quadriceps femoris sections from age-matched wild-type and *bgn* null animals were mounted on the same slide and stained using antibodies against dystrophin (DYS), α-, β-, and γ-sarcoglycan (α-, β-, or γ-SG), α- and β-dystroglycan (α- or β-DG), and the laminin α2 chain (LN-2). The sarcolemmal expression levels of each of this subset of DAPC proteins are unchanged in *bgn* null muscle. Results are representative of 6 pairs of 5-wk-old wild-type and *bgn* null muscles. Scale bar = 20 μm.

laminin α2. As shown in **Fig. 2**, immunofluorescent staining of muscle sections revealed that the sarcolemmal expression of dystrophin and α-, β-, and γ-sarcoglycan is unchanged in *bgn* null animals. The expression of α- and β-dystroglycan and the α2 chain of laminin were also indistinguishable between wild-type and *bgn* null muscle (Fig. 2).

We next used immunohistochemistry to examine the expression of the intracellular DAPC proteins involved in signaling and scaffolding: the dystrobrevins, syntrophins, and nNOS. In each experiment we also immunostained for dystrophin, which is unchanged and thus serves as an internal, positive control (Fig. 2 and **Fig. 3*A, B***). As shown in Fig. 3*A*, α-dystrobrevin-1 and -2 are expressed strongly at the muscle sarcolemma of wild-type muscle. Moreover, these proteins are localized in a continuous, uninterrupted distribution at the sarcolemma. In contrast, in *bgn* null muscle, α-dystrobrevin-1 and -2 are expressed at a lower level at the sarcolemma and are distributed in an irregular, punctate pattern.

We also observed that α-syntrophin and β1-syntrophin are reduced at the sarcolemma in *bgn*-deficient animals (Fig. 3*A*). The reduction in β1-syntrophin at the sarcolemma was pronounced, while that of α-syntrophin was subtler. On the other hand, the expression of β2-syntrophin at the sarcolemma of *bgn* null muscle did not differ from wild-type. The intracellular level of all three syntrophins was increased in *bgn* null compared to wild-type muscle (Fig. 3*A, B*).

Finally, nNOS has been shown to coimmunoprecipitate with α-syntrophin and to be lost at the sarcolemma of α-syntrophin-null muscle (19, 20). Therefore, we asked whether the skeletal muscle expression of nNOS is altered in *bgn* knockouts. As shown in Fig. 3*A*, sarcolemmal nNOS levels were lower in *bgn* null muscle than in wild-type. Taken together, these results demonstrate that there is a selective reduction in the expression of the dystrobrevin-syntrophin-nNOS complex in the sarcolemma of *bgn* null mice.

Virtually all components of the DAPC are expressed at the neuromuscular junction, with many being selectively enriched at this site. In addition, individuals with denervation disorders show specific changes in the expression patterns of the syntrophins and dystrobrevins, but not the rest of the DAPC (21). We thus asked whether expression of the α-dystrobrevins, syntrophins, and nNOS was altered at the synapse in *bgn* null muscle. The expression of each of these proteins was compared to that of ACh receptors, whose levels are unaffected by the loss of biglycan. We find that the expression levels and distribution of α-dystrobrevin-1, α-dystrobrevin-2, α-syntrophin, β1-syntrophin, β2-syntrophin, and nNOS

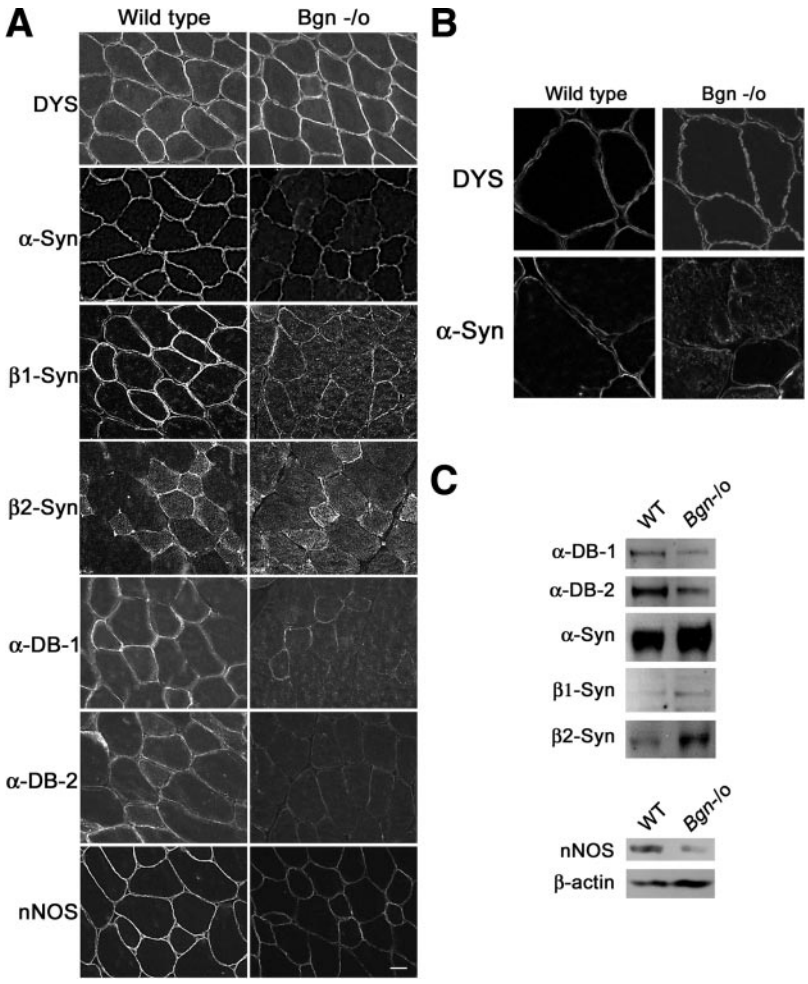

Figure 3. Expression of dystrobrevins, nNOS, and syntrophins in wild-type and *bgn* null skeletal muscle sections and microsomal membrane fractions. Quadriceps femoris sections from 5-wk-old wild-type and *bgn* null (*bgn* -/o) animals were stained using the indicated antibodies. Results are representative of 6 pairs of 5-wk-old wild-type and *bgn* null muscles. *A)* As shown in Fig. 2, the levels of dystrophin are indistinguishable in the wild-type and *bgn* null muscle. In contrast, there is a selective reduction of α-dystrobrevin-1 (α-DB-1), α-dystrobrevin-2 (α-DB-2), α-syntrophin (α-Syn), β1-syntrophin (β1-Syn), and nNOS at the sarcolemma of *bgn* null muscle. *B)* Higher magnification images of wild-type and *bgn* null quadriceps femoris sections stained using the indicated antibodies. The intracellular levels of α-syntrophin are increased in the biglycan null compared to the wild-type muscle. The intracellular levels of dystrophin (DYS) remain unchanged. Scale bar = 20 μm. *C)* A comparison of expression of the dystrobrevins, syntrophins, and nNOS in KCl-washed microsomal membranes from wild-type and *bgn* null muscle. Ten μg of membrane proteins from 5-wk-old quadriceps femoris muscles from wild-type and *bgn* null animals were separated by SDS-PAGE and immunoblotted with antibodies against α-dystrobrevin-1 (α-DB-1), α-dystrobrevin-2 (α-DB-2), α-syntrophin (α-Syn), β1-syntrophin (β1-Syn), and β2-syntrophin (β2-Syn). The expression levels of α-DB-1 and α-DB-2 are decreased in *bgn* null microsomes, while the levels of α-Syn, β1-Syn, and β2-Syn are increased. Proteins (10 μg) from non-KCl-washed microsomal membranes isolated from 5-wk-old quadriceps femoris muscles from wild-type and *bgn* null animals were separated via SDS-PAGE and immunoblotted using antibodies against nNOS and β-actin (loading control). Note the selective decrease in nNOS expression in *bgn* null muscle membranes. Similar results were obtained in membrane fractions obtained from 3 pairs of wild-type and *bgn* null muscles.

remain unchanged in *bgn* null neuromuscular junctions (data not shown). Thus, this DAPC subcomplex is reduced at the sarcolemma but maintained at the neuromuscular junction.

Dysregulation of α-dystrobrevin-1 and -2, α-, β1-, and β2-syntrophin, and nNOS content in membrane fractions from *bgn* null muscle

The immunohistochemical data described above indicate that the levels of α-dystrobrevin-1 and -2 are reduced at the plasma membrane of biglycan-deficient muscle fibers. To determine whether the biochemical profile of these proteins is also changed, we assessed their levels in KCl-washed heavy microsomal membrane fractions, which are a mixture of plasma and intracellular membranes (22). To compare the levels of membrane-associated dystrobrevin, we isolated fractions from wild-type and *bgn* null quadriceps muscle and probed them using a pan-specific anti-dystrobrevin Ab. Figure 3*C* shows that the levels of both α-dystrobrevin-1 and -2 are reduced in these membrane fractions.

We next examined the expression of α-, β1-, and β2-syntrophins in KCl-washed membrane fractions. Immunoblotting with isoform-specific antibodies revealed that the levels of all three syntrophins were increased in membrane fractions from *bgn* knockouts compared to wild-type controls (Fig. 3*C*). This increased expression is likely to reflect the contribution of syntrophins associated with intracellular membranes; indeed, it is in agreement with our immunohistochemical results showing elevated intracellular levels of all syntrophins in the *bgn* null muscle (Fig. 3*A, B*). These findings suggest that biglycan serves to appropriately target syntrophins to the muscle cell surface and/or to regulate the intracellular trafficking of these molecules.

We also compared the expression of nNOS in wild-type and *bgn* null quadriceps. Since KCl treatment strips nNOS from muscle membrane fractions (20), we isolated heavy microsomal membrane fractions with no KCl wash. As shown in Fig. 3*C*, the expression levels of nNOS at the membranes of *bgn* null animals are decreased compared to wild-type, in agreement with the immunohistochemical results.

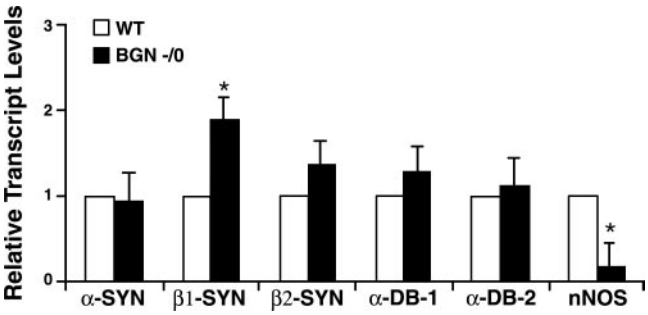

Figure 4. Relative mRNA expression of dystrobrevins, syntrophins, and nNOS in wild-type and *bgn* null skeletal muscle. Expression levels of the mRNAs encoding components of the dystrobrevin-syntrophin-nNOS complex in 5-wk-old *bgn* knockout quadriceps femoris muscle are shown relative to wild-type. Levels were determined by quantitative real-time PCR and are normalized to the expression levels of ATP synthase. *The changes in β1-syntrophin and nNOS transcript levels are statistically significant ($P<0.03$; Student's t test). $n = 3$.

Selective changes in β1-syntrophin and nNOS mRNA expression levels in skeletal muscle of *bgn* null mice

We next asked whether the changes in the expression of syntrophin-dystrobrevin-nNOS complex members observed in *bgn* null was reflected in changes transcript levels (**Fig. 4**). Quantitative real-time PCR (qRT-PCR) analysis showed that β1-syntrophin transcripts are significantly up-regulated in the *bgn* knockout compared to the wild-type (1.88±0.27 vs. 1.00, $P<0.03$; Student's t test), while nNOS message levels are down-regulated (0.18±0.27 vs. 1.00, $P<0.03$; Student's t test). On the other hand, the levels of both α-dystrobrevins and of α- and β2-syntrophin messages are equivalent in wild-type and *bgn* null muscle.

Biglycan induces the redistribution of nNOS to the plasma membrane

We next developed a cell culture system to further examine the role of biglycan in targeting DAPC components to the cell surface. We cultured biglycan-deficient myotubes and incubated them with either purified recombinant biglycan core polypeptide or with vehicle alone for 4 h. Living myotubes were labeled with rhodamine-α-bungarotoxin to visualize AChRs and to demarcate the plasma membrane. We then fixed and permeabilized the cells and immunostained for dystrobrevins, syntrophins, and nNOS. As shown in **Fig. 5*A***, nNOS is distributed throughout the cytoplasm in untreated cells, with little labeling observed in the region of the plasma membrane. However, biglycan treatment increases the levels of nNOS localized subadjacent to the myotube surface. We quantified this redistribution of nNOS by assigning each cell a score (0–4, 0 being no nNOS at the myotube surface, 4 being the highest change in nNOS at the surface; scored blind to treatment conditions) representing the extent to which surface nNOS was present. In the absence of biglycan, the mean score was 2.0 ± 0.11; in the presence of biglycan, the mean score was 2.94 ± 0.12. The histogram in Fig. 5*B* displays the number of untreated or biglycan-treated cells receiving each score. These data demonstrate that the treatment of *bgn* null myotubes with biglycan core increases the amount of nNOS on the myotube plasma membrane ($P<0.01$; Kolmogorov-Smirnov test).

In parallel experiments, we noted that α-dystrobrevin -1 and -2 and β2-syntrophin staining were widely expressed within the cell, but little cell surface-proximal expression was detected. On the other hand, α-syntrophin and β1-syntrophin were expressed throughout the

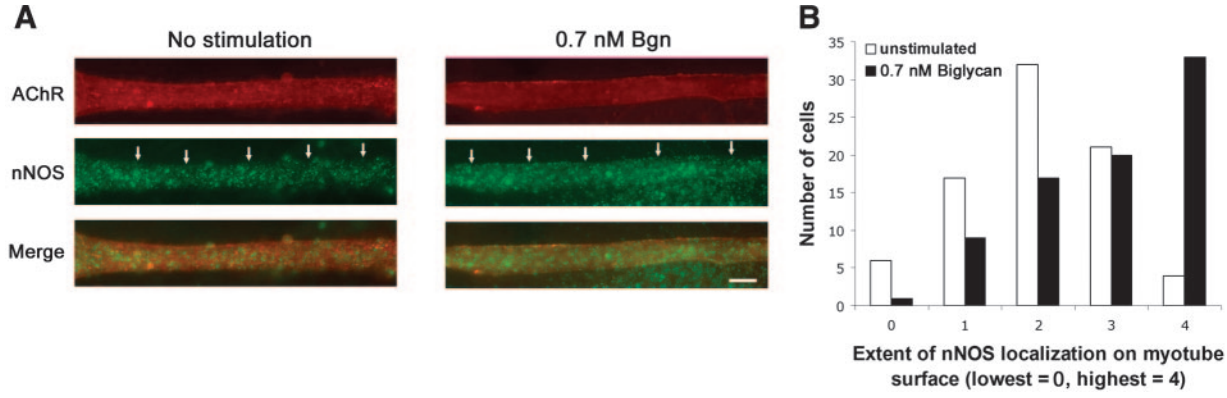

Figure 5. Biglycan treatment regulates the localization of nNOS in cultured myotubes. *A)* Differentiated myotubes deficient in biglycan expression were treated with medium alone or with 0.7 nM recombinant biglycan core polypeptide for 4 h. Living myotubes were then labeled with rh-α-bungarotoxin to label surface AChRs (red). The myotubes were then fixed, permeabilized, and stained for nNOS (green). Arrows delineate the myotube plasma membrane. In the absence of biglycan, nNOS expression is largely cytosolic. Upon biglycan treatment, nNOS becomes more highly localized to the plasma membrane. *B)* Quantification of biglycan-induced nNOS relocalization. Myotubes were scored blind to treatment conditions on a scale of 0 to 4 (0 being no nNOS cell surface expression, 1 being low nNOS cell surface expression and 4 being high nNOS cell surface expression). The number of untreated and *bgn* null cells receiving each score was graphed. The number of biglycan-treated myotubes displaying cell surface localization of nNOS was significantly higher than the number of untreated myotubes with nNOS on their surface ($P<0.01$, Kolmogorov-Smirnov test).

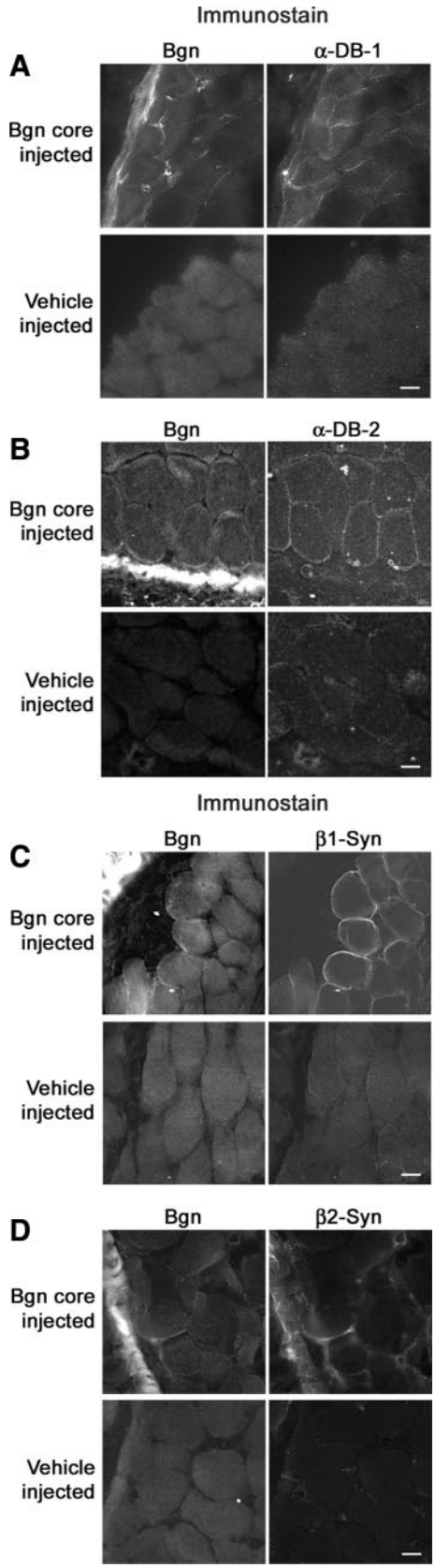

Figure 6. Intramuscular injection of biglycan core polypeptide into *bgn* null skeletal muscle restores sarcolemmal expression of α-dystrobrevin-1 and -2 and β1- and β2-syntrophin. Exogenous biglycan core polypeptide increases the sarcolemmal expression of α-dystrobrevin-1 and -2 and β1- and β2-syntrophin *in vivo*. Two-wk-old *bgn* null mice were injected i.m. into the right quadriceps femoris muscles with 50 μg biglycan core, and into the left quadriceps with buffer alone. 1.0% India ink was added to each injected solution to allow visualization of the injection site. Muscle was harvested 11 days after injection, sectioned, and immunolabeled. Biglycan core polypeptide enhances sarcolemmal expression of α-dystrobrevin-1 (α-DB-1) (*A*), α-dystrobrevin-2 (α-DB-2) (*B*), β1-syntrophin (β1-Syn) (*C*), and β2-syntrophin (β2-Syn) (*D*). The injected biglycan core polypeptide colocalizes with α-dystrobrevin and β-syntrophin expression at the sarcolemma of injected muscle. Scale bar = 20 μM.

cell, including in a surface-proximal disposition. However, biglycan treatment did not alter the localization of these proteins.

The injection of purified biglycan protein restores the expression of α-dystrobrevins and β-syntrophins to the sarcolemma of *bgn* null muscle fibers *in vivo*

The results described above show that a subcomplex of the DAPC is reduced at the sarcolemma of adult *bgn* null mice. However, since biglycan is absent throughout development, it is not possible to determine when biglycan is playing a role in the localization of these components. Moreover, since biglycan is expressed in other locales, including bone and tendon (23, 24), it is possible that the muscle phenotype is secondary to a defect in another tissue. Finally, the results with the *bgn* null mice do not allow a determination of which biglycan form(s) (core or proteoglycan) is required for directing the correct localization of the DAPC subcomplex.

To address these questions, we asked whether i.m. injection of purified biglycan core or proteoglycan could restore the expression of the syntrophin-dystrobrevin-nNOS DAPC subcomplex to the sarcolemma of *bgn* null mice. Purified recombinant biglycan core polypeptide or proteoglycan (50 μg) was injected into the right quadriceps femoris muscles of 2-wk-old *bgn* null animals. Buffer alone was injected into the left quadriceps to provide intra-animal comparisons. The injection site was visualized by the inclusion of India ink in each solution. Quadriceps were dissected 4, 7, 11, and 14 days postinjection, sectioned, and immunostained. As shown in **Fig. 6*A–D*** (upper left), i.m. injected biglycan core polypeptide becomes stably associated with the perimysium and sarcolemma, persisting for up to 14 days after a single injection. Intramuscularly injected biglycan proteoglycan also becomes stably associated with the perimysium (data not shown). No biglycan immunoreactivity was observed on the vehicle-injected side at any time examined (Fig. 6*A–D*, lower left).

Intramuscularly injected biglycan core had a striking effect on the expression of the syntrophins and dystrobrevins in the *bgn* null muscle. By 11 days postinjection, we observed increased α-dystrobrevin-1 and -2 and β1- and β2-syntrophin expression at the sarcolemma. Moreover, the increased expression of these intracellu-

lar DAPC proteins showed a tight spatial correlation with the exogenous biglycan (Fig. 6*A–D*; compare upper left and upper right). No up-regulation was observed in the vehicle-injected muscle (Fig. 6*A–D*; compare upper and lower right) or in the biglycan proteoglycan-injected muscle (data not shown). The increase in α-dystrobrevin-1 and -2 and β1- and β2-syntrophin persisted at 14 days postinjection. We did not observe a change in α-syntrophin after biglycan injection. Additionally, nNOS expression was increased at the injection sites of both biglycan-treated and vehicle-treated muscle, suggesting that nNOS expression increases after mechanical injury. Indeed, there is evidence that mechanical injury induces nNOS expression in the brain (25). Taken together, these results show that biglycan can be delivered to muscle *in vivo* and that it can direct the localization of the α-dystrobrevins and β-syntrophins to the sarcolemma. Moreover, this activity is a property of the biglycan core polypeptide and does not require the GAG side chains. Thus, biglycan can regulate the expression of the dystrobrevin-syntrophin complex at the sarcolemma *in vivo*.

DISCUSSION

In this study we demonstrate that *bgn* null mice have a mild muscular dystrophy and provide several lines of evidence that this extracellular protein regulates the localization and expression of a subset of intracellular DAPC components in skeletal muscle. Moreover, our data indicate that the mechanisms underlying the biglycan-mediated sarcolemmal expression of the syntrophins, dystrobrevins, and nNOS are likely to be distinct. Here we discuss the evidence supporting these conclusions, the potential underlying mechanisms, and the implications of these findings for potential therapies for muscular dystrophy.

Bgn null muscle displays a mild muscular dystrophy characterized by elevated serum CK and Evans blue dye uptake, increased numbers of centrally nucleated fibers, and abnormal myofiber size distribution. The diaphragm was most affected, with ~10% of the fibers showing central nuclei. These features observed at 5 wk of age were not progressive and were not accompanied by mononuclear cell infiltration. It is noteworthy that this phenotype is qualitatively similar to that observed in α-dystrobrevin null mice (which also show reduced nNOS at the sarcolemma; ref 26). In that case ~50% central nuclei are observed, but little mononuclear infiltration was seen and the overall dystrophy is considerably less severe than in *mdx*. α-Syntrophin knockout mice show decreased sarcolemmal expression of α-dystrobrevin-2 and nNOS, but no myopathic symptoms (27, 28). Finally, α-dystrobrevin-1 has been shown to bind to the intermediate filament proteins desmuslin and syncoilin [Newey, 2001; Blake, 2002]. It is therefore possible that the dystrobrevins help protect muscle cell membranes from contraction-induced damage by structurally linking the DAPC to the cytoskeleton. Together these findings suggest that the reduced levels of α-dystrobrevin, at least in part, underlie the dystrophic phenotype observed in the *bgn* null mice.

Our results indicate that distinct mechanisms underlie the reduction of dystrobrevins, syntrophins, and nNOS at the sarcolemma in *bgn* null mice. Both immunohistochemical staining and Western blots of total muscle membranes show reductions in α-dystrobrevin-1 and -2 (Fig. 3). Moreover, the transcript levels are unchanged (Fig. 4). At present it is not known whether this post-transcriptional reduction of dystrobrevin is due to increased degradation or decreased translation. Since the levels of dystrophin are unchanged in these mice, the reduction in dystrobrevin could be due to nondystrophin-mediated association with the membrane (28–30) and/or to defective signaling. On the other hand, nNOS seems likely to be regulated at the transcriptional level *in vivo*, since mRNA encoding this protein is reduced >5-fold compared to controls. *Bgn* could also regulate nNOS targeting, since acute treatment of myotubes with purified biglycan induces and increase in the plasma membrane-association of this enzyme. However, it should be stressed that the *in vivo* and the cell culture experiments are quite different. For example, the DAPC in cultured myotubes is rudimentary at best, with a fragmentary basal lamina, and substantial intracellular expression of nNOS and sarcoglycans (29, 31).

The dysregulation of syntrophins in *bgn* null mice is complex. All of the syntrophins show defective intracellular trafficking as evidenced by increased intracellular localization and elevated expression in KCl-washed membranes. The intracellular accumulation of the syntrophins suggests that these proteins are targeted to the muscle membrane via a different mechanism than that used by the rest of the DAPC. Indeed, previous work has indeed shown that dystrophin and syntrophin take different routes during targeting to the membrane (32). Syntrophins are transported in post-Golgi vesicles that exocytose to fuse with the membrane, while dystrophin becomes directly associated with the sarcolemma after synthesis. The syntrophins also showed distinct transcriptional regulation: α- and β2-syntrophin messages were unchanged, while those encoding β1-mRNA were elevated (Fig. 4). Finally, the changes in sarcolemmal expression vary among the syntrophins: β1-syntrophin shows the most marked decrease, while α-syntrophin was less reduced and β2- was indistinguishable from wild-type. Thus, while all of the syntrophins are affected in the mutant mice, biglycan is particularly important for the regulation of β1-syntrophin.

The mechanism by which biglycan signals the sarcolemmal localization of the dystrobrevin-syntrophin subcomplex or prevents the intracellular accumulation of syntrophins is not known. Biglycan binds to α-dystroglycan via its GAG side chains (3). However, the biglycan core polypeptide is active in our cell culture and *in vivo* assays, suggesting that the effects observed are not

likely to be mediated by α-dystroglycan. In addition, since dystrophin expression is unchanged in biglycan-deficient muscle, it is unlikely that the loss of syntrophin and dystrobrevin binding sites on dystrophin is causing their mislocalization. The sarcoglycan complex can be purified with dystrobrevin and syntrophin in the absence of dystroglycan or dystrophin (31). Moreover, coimmunoprecipitation and ligand blot overlay experiments from our laboratory have demonstrated that biglycan's polypeptide core binds to α- and γ-sarcoglycan (H. Hagiwara, M. Rafii, and J. Fallon, unpublished observations). Thus, biglycan binding to sarcoglycans, perhaps in a complex that does not contain dystrophin, could form part of the transmembrane complex by which this matrix protein regulates the localization of the dystrobrevin-syntrophin-nNOS complex.

Finally, we show that i.m. administration of purified biglycan core polypeptide can restore the sarcolemmal expression of α-dystrobrevin-1 and -2, and β1- and β2-syntrophin in *bgn* null mice. This result demonstrates that biglycan can directly induce an increase in protein expression and/or a relocalization of DAPC proteins from the cytoplasm to the plasma membrane. It also demonstrates that i.m. injected biglycan protein appropriately localizes to the perimysium and sarcolemma and is stably associated with these sites for up to 2 wk after administration. These pharmacokinetic properties of biglycan, coupled with its ability to induce specific changes in the localization of some DAPC components in muscle, suggest that it is a potential therapeutic for muscular dystrophy. It will be of interest to determine whether the administration of biglycan to dystrophin or dystrophin/utrophin knockout mice induces the appropriate expression and localization of DAPC proteins, and ameliorates the dystrophic symptoms of these mutants. FJ

We thank Beth McKechnie for superb technical assistance. This work was supported by grants from the NIH (J.F., HD23924 and RR15578; D.M., AR42826, R44 NS045432; S.F., NS33145, and NS4678, A.R.A. was supported by T32MH20068).

REFERENCES

1. Metzinger, L., Blake, D. J., Squier, M. V., Anderson, L. V., Deconinck, A. E., Nawrotzki, R., Hilton-Jones, D., and Davies, K. E. (1997) Dystrobrevin deficiency at the sarcolemma of patients with muscular dystrophy. *Hum. Mol. Genet.* **6,** 1185–1191
2. Blake, D. J., Weir, A., Newey, S. E., and Davies, K. E. (2002) Function and genetics of dystrophin and dystrophin-related proteins in muscle. *Physiol. Rev.* **82,** 291–329
3. Bowe, M. A., Mendis, D. B., and Fallon, J. R. (2000) The small leucine-rich repeat proteoglycan biglycan binds to alpha-dystroglycan and is upregulated in dystrophic muscle. *J. Cell Biol.* **148,** 801–810
4. Ahn, A. H., and Kunkel, L. M. (1993) The structural and functional diversity of dystrophin. [Review]. *Nat. Genet.* **3,** 283–291
5. Cohn, R. D., and Campbell, K. P. (2000) Molecular basis of muscular dystrophies. *Muscle Nerve* **23,** 1456–1471
6. Xu, T., Bianco, P., Fisher, L. W., Longenecker, G., Smith, E., Goldstein, S., Bonadio, J., Boskey, A., Heegaard, A. M., Sommer, B., Satomura, K., Dominguez, P., Zhao, C., Kulkarni, A. B., Robey, P. G., and Young, M. F. (1998) Targeted disruption of the biglycan gene leads to an osteoporosis-like phenotype in mice. *Nat. Genet.* **20,** 78–82
7. Ameye, L., and Young, M. F. (2002) Mice deficient in small leucine-rich proteoglycans: novel in vivo models for osteoporosis, osteoarthritis, Ehlers-Danlos syndrome, muscular dystrophy, and corneal diseases. *Glycobiology* **12,**107R–116R
8. Casar, J. C., McKechnie, B. A., Fallon, J. R., Young, M. F., and Brandan, E. (2004) Transient up-regulation of biglycan during skeletal muscle regeneration: delayed fiber growth along with decorin increase in biglycan-deficient mice. *Dev. Biol.* **268,** 358–371
9. Hayashi, Y., Liu, C. Y., Jester, J. J., Hayashi, M., Wang, I. J., Funderburgh, J. L., Saika, S., Roughley, P. J., Kao, C. W., and Kao, W. W. (2005) Excess biglycan causes eyelid malformation by perturbing muscle development and TGF-alpha signaling. *Dev. Biol.* **277,** 222–234
10. Hocking, A. M., Strugnell, R. A., Ramamurthy, P., and McQuillan, D. J. (1996) Eukaryotic expression of recombinant biglycan. Post-translational processing and the importance of secondary structure for biological activity. *J. Biol. Chem.* **271,** 19571–19577
11. Peters, M. F., Adams, M. E., and Froehner, S. C. (1997) Differential association of syntrophin pairs with the dystrophin complex. *J. Cell Biol.* **138,** 81–93
12. Peters, M. F., Sadoulet-Puccio, H. M., Grady, M. R., Kramarcy, N. R., Kunkel, L. M., Sanes, J. R., Sealock, R., and Froehner, S. C. (1998) Differential membrane localization and intermolecular associations of alpha-dystrobrevin isoforms in skeletal muscle. *J. Cell Biol.* **142,** 1269–1278
13. Ramamurthy, P., Hocking, A. M., and McQuillan, D. J. (1996) Recombinant decorin glycoforms. Purification and structure. *J. Biol. Chem.* **271,** 19578–19584
14. Goldberg, M., Septier, D., Rapoport, O., Iozzo, R. V., Young, M. F., and Ameye, L. G. (2005) Targeted disruption of two small leucine-rich proteoglycans, biglycan and decorin, excerpts divergent effects on enamel and dentin formation. *Calcified Tissue Int.* **77,** 297–310
15. Winer, J., Jung, C. K., Shackel, I., and Williams, P. M. (1999) Development and validation of real-time quantitative reverse transcriptase-polymerase chain reaction for monitoring gene expression in cardiac myocytes in vitro. *Analyt. Biochem.* **270,** 41–49
16. Morgan, J. E., Beauchamp, J. R., Pagel, C. N., Peckham, M., Ataliotis, P., Jat, P. S., Noble, M. D., Farmer, K., and Partridge, T. A. (1994) Myogenic cell lines derived from transgenic mice carrying a thermolabile T antigen: a model system for the derivation of tissue-specific and mutation-specific cell lines. *Dev. Biol.* **162,** 486–498
17. Hack, A. A., Groh, M. E., and McNally, E. M. (2000) Sarcoglycans in muscular dystrophy. *Microsc. Res. Tech.* **48,** 167–180
18. Matsuda, R., Nishikawa, A., and Tanaka, H. (1995) Visualization of dystrophic muscle fibers in Mdx mouse by vital staining with Evans blue: evidence of apoptosis in dystrophin-deficient muscle. *J Biochem. Tokyo* **118,** 959–964
19. Brenman, J. E., Chao, D. S., Gee, S. H., Mcgee, A. W., Craven, S. E., Santillano, D. R., Wu, Z. Q., Huang, F., Xia, H. H., Peters, M. F., Froehner, S. C., and Bredt, D. S. (1996) Interaction of nitric oxide synthase with the postsynaptic density protein PSD-95 and alpha 1-syntrophin mediated by PDZ domains. *Cell* **84,** 757–767
20. Kameya, S., Miyagoe, Y., Nonaka, I., Ikemoto, T., Endo, M., Hanaoka, K., Nabeshima, Y., and Takeda, S. (1999) alpha1-syntrophin gene disruption results in the absence of neuronal-type nitric-oxide synthase at the sarcolemma but does not induce muscle degeneration. *J. Biol. Chem.* **274,** 2193–2200
21. Compton, A. G., Cooper, S. T., Hill, P. M., Yang, N., Froehner, S. C., and North, K. N. (2005) The syntrophin-dystrobrevin subcomplex in human neuromuscular disorders. *J. Neuropathol. Exp. Neurol.* **64,** 350–361
22. Mitchell, R., Palade, P., and Fleischer, S. (1983) Purification of morphologically intact triad structures from skeletal muscle. *J. Cell Biol.* **96,** 1008–1016
23. Fisher, L. W., Termine, J. D., and Young, M. F. (1989) Deduced protein sequence of bone small proteoglycan I (biglycan) shows homology with proteoglycan II (decorin) and several nonconnective tissue proteins in a variety of species. *J. Biol. Chem.* **264,** 4571–4576

24. Rees, S. G., Flannery, C. R., Little, C. B., Hughes, C. E., Caterson, B., and Dent, C. M. (2000) Catabolism of aggrecan, decorin and biglycan in tendon. *Biochem. J.* **350,** 181–188
25. Saxon, D. W., and Beitz, A. J. (1994) Cerebellar injury induces NOS in Purkinje cells and cerebellar afferent neurons. *NeuroReport* **5,** 809–812
26. Grady, R. M., Grange, R. W., Lau, K. S., Maimone, M. M., Nichol, M. C., Stull, J. T., and Sanes, J. R. (1999) Role for alpha-dystrobrevin in the pathogenesis of dystrophin-dependent muscular dystrophies. *Nat. Cell Biol.* **1,** 215–220
27. Adams, M. E., Kramarcy, N., Krall, S. P., Rossi, S. G., Rotundo, R. L., Sealock, R., and Froehner, S. C. (2000) Absence of alpha-syntrophin leads to structurally aberrant neuromuscular synapses deficient in utrophin. *J. Cell Biol.* **150,** 1385–1398
28. Crawford, G. E., Faulkner, J. A., Crosbie, R. H., Campbell, K. P., Froehner, S. C., and Chamberlain, J. S. (2000) Assembly of the dystrophin-associated protein complex does not require the dystrophin COOH-terminal domain. *J. Cell Biol.* **150,** 1399–1410
29. Abdelmoity, A., Padre, R. C., Burzynski, K. E., Stull, J. T., and Lau, K. S. (2000) Neuronal nitric oxide synthase localizes through multiple structural motifs to the sarcolemma in mouse myotubes. *FEBS Lett.* **482,** 65–70
30. Crosbie, R. H., Barresi, R., and Campbell, K. P. (2002) Loss of sarcolemma nNOS in sarcoglycan-deficient muscle. *FASEB J.* **16,** 1786–1791
31. Yoshida, M., Hama, H., Ishikawa-Sakurai, M., Imamura, M., Mizuno, Y., Araishi, K., Wakabayashi-Takai, E., Noguchi, S., Sasaoka, T., and Ozawa, E. (2000) Biochemical evidence for association of dystrobrevin with the sarcoglycan-sarcospan complex as a basis for understanding sarcoglycanopathy. *Hum. Mol. Genet.* **9,** 1033–1040
32. Marchand, S., Stetzkowski-Marden, F., and Cartaud, J. (2001) Differential targeting of components of the dystrophin complex to the postsynaptic membrane. *Eur. J. Neurosci.* **13,** 221–229

Received for publication September 28, 2005.
Accepted for publication March 31, 2006.

Biglycan regulates the expression and sarcolemmal localization of dystrobrevin, syntrophin, and nNOS

Mary Lynn Mercado,* Alison R. Amenta,* Hiroki Hagiwara,* Michael S. Rafii,* Beatrice E. Lechner,* Rick T. Owens,† David J. McQuillan,† Stanley C. Froehner,‡ and Justin R. Fallon*,[1]

*Department of Neuroscience, Brown University, Providence, Rhode Island, USA; †LifeCell Corporation, Branchburg, New Jersey, USA; and ‡Department of Physiology and Biophysics, University of Washington, Seattle, Washington, USA

To read the full text of this article, go to http://www.fasebj.org/cgi/doi/10.1096/fj.05-5124fje

SPECIFIC AIMS

Defects in the dystrophin-associated protein complex (DAPC) are the cause of most muscular dystrophies. The aims of this study were to *1)* determine the function of the extracellular matrix proteoglycan biglycan in regulating the composition of the DAPC at the myofiber plasma membrane and *2)* test the potential of biglycan as a therapeutic for muscular dystrophy.

PRINCIPAL FINDINGS

1. Biglycan null mice display a dystrophic phenotype

Mutations in any one of several DAPC components cause a wide range of muscular dystrophies. In previous work we have shown that biglycan binds to the DAPC component α-dystroglycan. Therefore, we tested whether biglycan null mice display a dystrophic phenotype. First, we performed the Evans blue dye uptake assay to determine whether muscle membrane integrity is compromised in the biglycan null mice. We intravenously injected wild-type, biglycan null (*bgn*), and dystrophin-null (*mdx*) mice with Evans blue dye, and the extent of uptake into quadriceps femoris muscle fibers was assessed. Wild-type fibers exhibited very little dye uptake, *mdx* fibers exhibited almost complete uptake, and *bgn* fibers exhibited an intermediate perimembranous uptake. Next we examined the muscles of *bgn* mice histologically. A fraction of the myofibers in *bgn* null mice displayed centrally localized nuclei, a hallmark of regenerated fibers (5.08%±0.58 and 9.65%±1.34 in quadriceps and diaphragm, respectively). We did not observe extensive necrosis or mononuclear cell infiltration. Finally, we measured fiber diameters from quadriceps femoris, gastrocnemius, and diaphragm muscles. In the quadriceps and gastrocnemius, *bgn* null fibers were smaller than wild-type fibers. On the other hand, the diaphragm of biglycan null mice displayed a wider fiber size distribution. These results indicate that *bgn* muscle is mildly dystrophic, with increased membrane permeability and an increased number of fibers that have undergone degeneration and regeneration.

2. α-Dystrobrevin, syntrophin, and nNOS expression is selectively reduced at the sarcolemma of *bgn* mice

We next compared the expression of individual DAPC proteins in the quadriceps femoris muscles of adult wild-type and *bgn* null mice. In all cases we compared biglycan null mice to either wild-type littermates or to congenic, age-matched wild-type animals. Sarcolemmal expression of the α2 chain of laminin, α- and β-dystroglycan, α-, β-, and γ-sarcoglycan and dystrophin was equivalent in wild-type and *bgn* null animals. However, expression levels of α-dystrobrevin-1 and -2, α- and β1-syntrophin and nNOS were reduced at the sarcolemma of *bgn* mice (**Fig. 1*A***). In addition, we observed an increase in the intracellular staining of α- and β2-syntrophin in the larger diameter fibers and an increase in cytosolic β1-syntrophin in every fiber of the *bgn* knockouts (Fig. 1*A*, *B*).

We also biochemically compared the expression levels of the α-dystrobrevins and syntrophins in KCl-washed heavy microsomal membrane fractions (a mixture of plasma and intracellular membranes). The membrane-associated expression of α-dystrobrevin-1 and -2 was decreased overall in *bgn* muscle. Conversely, levels of α-, β1-, and β2-syntrophin were increased in the membrane fractions of *bgn* mice. The increase in syntrophins in these total membrane fractions is in accord with the increase in intracellular syntrophin expression seen via immunohistochemistry (Fig. 1*C*). Finally, we compared nNOS expression between non-KCl-washed membrane fractions from wild-type and *bgn* muscle. nNOS expression was reduced in the *bgn* membrane fractions (Fig. 1*D*).

[1]Correspondence: Department of Neuroscience, Brown Univrsity, 190 Thayer St., Box 1953, Providence, RI 02912, USA. E-mail: Justin_Fallon@brown.edu

doi: 10.1096/fj.05–5124fje

0892-6638/06/0020-1724 © FASEB

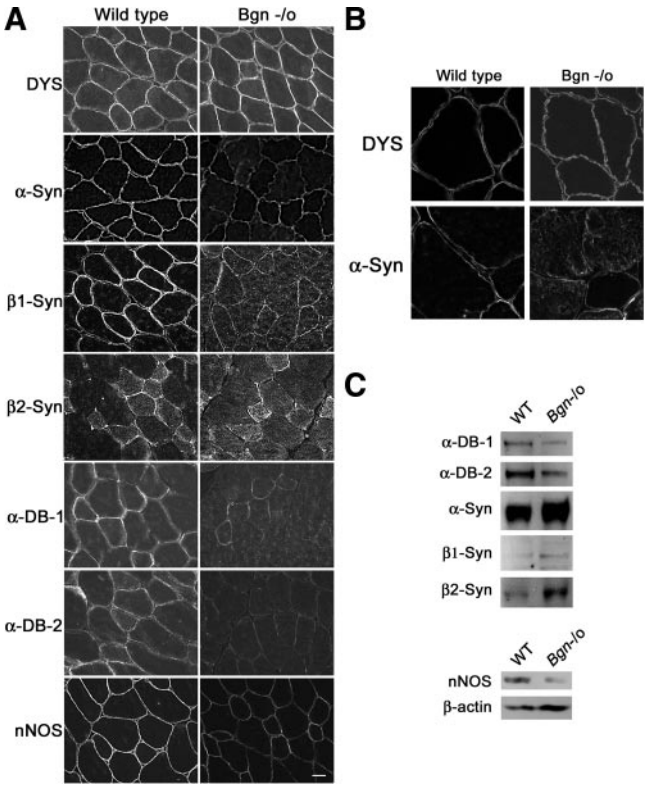

Figure 1. Expression of dystrobrevins, nNOS, and syntrophins in wild-type and *bgn* null skeletal muscle sections and microsomal membrane fractions. Quadriceps femoris sections from 5-wk-old wild-type and *bgn* null (*bgn* -/o) animals were stained using the indicated antibodies. The experiment was repeated six times, using animals from 6 litters. *A)* The levels of dystrophin are indistinguishable in wild-type and *bgn* null muscle. In contrast, there is a selective reduction of α-dystrobrevin-1 (α-DB-1), α-dystrobrevin-2 (α-DB-2), α-syntrophin (α-Syn), β1-syntrophin (β1-Syn), and nNOS at the sarcolemma of *bgn* null muscle. *B)* Higher magnification images of wild-type and *bgn* null quadriceps femoris sections stained using the indicated antibodies. The intracellular levels of α-syntrophin are increased in the biglycan null compared with wild-type muscle. The intracellular levels of dystrophin (DYS) remain unchanged. Scale bar = 20 μm. *C)* A comparison of expression of the dystrobrevins, syntrophins, and nNOS in KCl-washed microsomal membranes from wild-type and *bgn* null muscle. 10 μg of membrane proteins from 5-wk-old quadriceps femoris muscles from wild-type and *bgn* null animals was separated by SDS-PAGE and immunoblotted with antibodies against α-dystrobrevin-1 (α-DB-1), α-dystrobrevin-2 (α-DB-2), α-syntrophin (α-Syn), β1-syntrophin (β1-Syn), and β2-syntrophin (β2-Syn). The expression levels of α-DB-1 and α-DB-2 are decreased in *bgn* null microsomes, while the levels of α-Syn, β1-Syn, and β2-Syn are increased. Proteins (10 μg) from non-KCl-washed microsomal membranes isolated from 5-wk-old quadriceps femoris muscles from wild-type and *bgn* null animals were separated via SDS-PAGE and immunoblotted using antibodies against nNOS and β-actin (as a loading control). Note the selective decrease in nNOS expression in *bgn* null muscle membranes.

3. Biglycan induces the redistribution of nNOS to the plasma membrane

We next developed a cell culture system to further examine the role of biglycan in targeting DAPC components to the cell surface. We cultured biglycan-deficient myotubes and incubated them with either purified recombinant biglycan core polypeptide (0.7 nM) or with vehicle alone for 4 h. Living myotubes were labeled with rhodamine-α-bungarotoxin to visualize AChRs and to demarcate the plasma membrane. We then fixed and permeabilized the cells and immunostained for nNOS. In untreated cells nNOS was distributed throughout the cytoplasm, with little labeling observed at the plasma membrane. Biglycan treatment increased nNOS levels at the myotube surface. We quantified this redistribution of nNOS by assigning each cell a score (1–4, 4 being the highest) representing the extent to which surface nNOS was present. In the absence of biglycan, the mean score was 2.0 ± 0.11, whereas in the presence of biglycan the mean score was 2.94 ± 0.12. These data demonstrate that treatment of

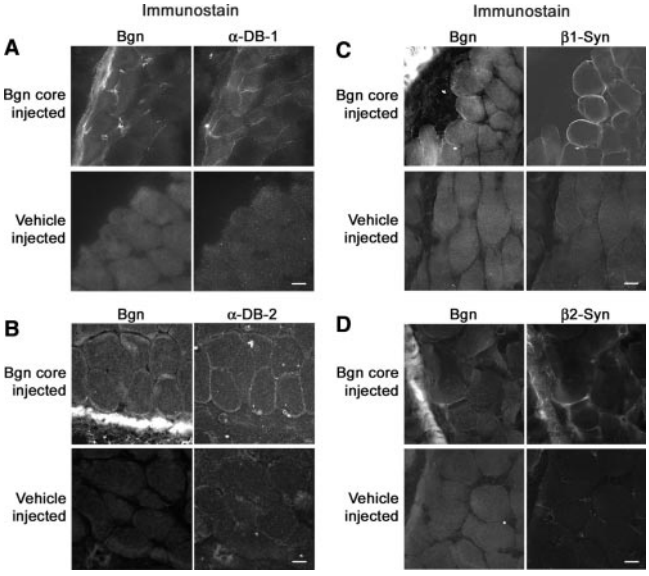

Figure 2. Intramuscular injection of biglycan core polypeptide into *bgn* null skeletal muscle restores sarcolemmal expression of α-dystrobrevin-1 and -2 and β1- and β2-syntrophin. Exogenous biglycan core polypeptide increases the sarcolemmal expression of α-dystrobrevin-1 and -2 and β1- and β2-syntrophin *in vivo*. Two-wk-old *bgn* null mice were injectedintramuscularly into the right quadriceps femoris muscles with 50 μg biglycan core and into the left quadriceps with buffer alone. 1.0% india ink was added to each injected solution to allow visualization of the injection site. Muscle was harvested 11 days after injection, sectioned, and immunolabeled. The injections were performed using three *bgn* null litters (14 animals total). Biglycan core polypeptide enhances sarcolemmal expression of α-dystrobrevin-1 (α-DB-1) (*A*), α-dystrobrevin-2 (α-DB-2) (*B*), β1-syntrophin (β1-Syn) (*C*), and β2-syntrophin (β2-Syn) (*D*). The injected biglycan core polypeptide colocalizes with α-dystrobrevin and β-syntrophin expression at the sarcolemma of injected muscle. Scale bar = 20 μM.

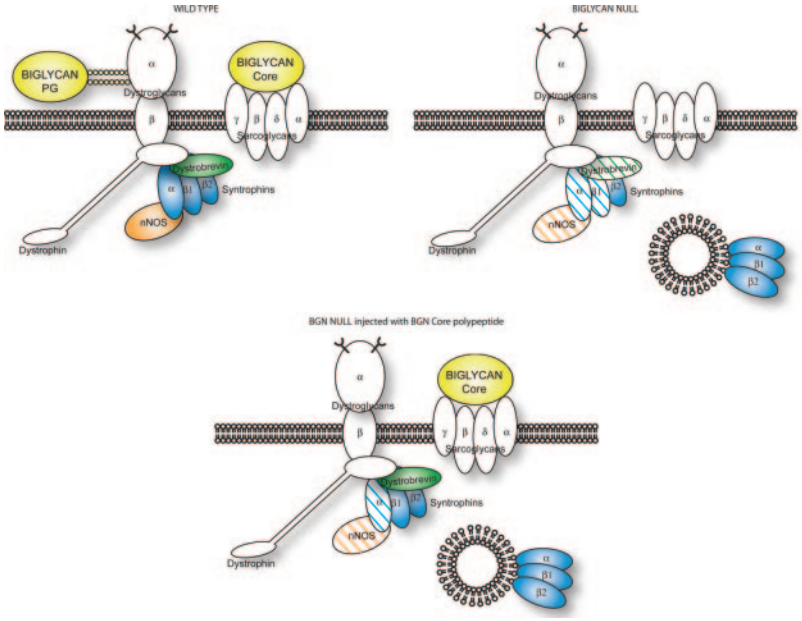

Figure 3. Biglycan regulates the sarcolemmal expression and membrane trafficking of the NODS complex proteins. In normal muscle, biglycan is expressed in a core polypeptide form as well as a proteoglycan form that binds to α-dystroglycan via its GAG side chains. In biglycan null animals the levels of dystrobrevins-1 and -2, α1- and β1-syntrophin and nNOS at the sarcolemma are reduced. Moreover, there is an increase in the level of syntrophins associated with intracellular membranes. Intramuscular injection of recombinant biglycan core polypeptide restores the sarcolemmal association of the dystrobrevins and β1/2 syntrophins.

biglycan null myotubes with biglycan core increases the amount of nNOS on the myotube plasma membrane ($P<0.01$; Kolmogorov-Smirnov test).

We also examined the localization of α-dystrobrevin-1 and -2, and α-, β1-, and β2-syntrophin in biglycan null myotubes in the absence or presence of biglycan. α-Dystrobrevin-1 and -2 and β2-syntrophin staining were widely expressed within the cell, but little cell surface proximal expression was detected. In contrast, α-syntrophin and β1-syntrophin were expressed throughout the cell including in a surface-proximal disposition. Biglycan treatment did not significantly alter the localization of these proteins.

4. The injection of purified biglycan protein restores the expression of α-dystrobrevins and β-syntrophins to the sarcolemma of *bgn* null muscle fibers *in vivo*

We asked whether intramuscular (i.m.) injection of *bgn* null mice with purified biglycan core polypeptide could directly restore the expression of the syntrophin-dystrobrevin-nNOS DAPC subcomplex to the sarcolemma. Purified recombinant biglycan core polypeptide (50 μg) was injected into the right quadriceps femoris muscles of 2-wk-old *bgn* null animals. Buffer alone was injected into the left quadriceps to provide intra-animal comparisons. The injection site was visualized by the inclusion of India ink in each solution. Quadriceps were dissected 4, 7, 11, and 14 days postinjection, sectioned, and immunostained. As shown in **Fig. 2*A–D*** (upper left), i.m. injected biglycan becomes stably associated with the perimysium and sarcolemma. No biglycan immunoreactivity was observed on the vehicle-injected side at any time (Fig. 2*A–D*, lower left). Eleven and 14 days after injection of biglycan we observed increased α-dystrobrevin-1 and -2 and β1- and β2-syntrophin expression at the sarcolemma. Moreover, the increased expression of these intracellular DAPC proteins showed a tight spatial correlation with the exogenous biglycan (Fig. 2*A–D*; compare upper left and upper right). No up-regulation was observed in the vehicle-injected muscle (Fig. 2*A–D*; compare upper and lower right). We did not observe a change in α-syntrophin or nNOS expression after biglycan injection. Thus, biglycan can be delivered to muscle *in vivo* and direct the localization of the α-dystrobrevins and β-syntrophins to the sarcolemma.

CONCLUSIONS AND SIGNIFICANCE

In this study we demonstrate that biglycan regulates the targeting of a specific subset of DAPC components—the syntrophin-dystrobrevin-nNOS complex—to the sarcolemma. The mechanism by which biglycan signals to localize this dystrobrevin-syntrophin subcomplex is unknown (**Fig. 3**). Intramuscular administration of purified biglycan core polypeptide can restore the sarcolemmal expression of α-dystrobrevin-1 and -2, and β1- and β2-syntrophin in biglycan null mice. This result demonstrates that biglycan can directly induce an increase in protein expression and/or a relocalization of DAPC proteins from the cytoplasm to the plasma membrane. It also shows that i.m. injected biglycan protein appropriately localizes to the perimysium and sarcolemma and is stably associated with these sites for up to 2 wk after administration. These pharmacokinetic properties of biglycan, coupled with its ability to induce specific changes in the localization of some DAPC components in muscle, suggest it is a potential therapy for muscular dystrophy. FJ